

Finite-temperature magnetism of $\text{Fe}_x\text{Pd}_{1-x}$ and $\text{Co}_x\text{Pt}_{1-x}$ alloys

S. Polesya^a, S. Mankovsky^a, O. Sipr^b, W. Meindl^c, C. Strunk^c, H. Ebert^a

^a *Department of Chem. and Biochem./Phys. Chem., LMU Munich,*

Butenandtstrasse 11, D-81377 Munich, Germany

^b *Institute of Physics AS CR, v. v. i.,*

Cukrovarnicka 10, 162 53 Praha, Czech Republic

^c *University Regensburg, D-93040 Regensburg, Germany*

(Dated: August 24, 2010)

Abstract

The finite-temperature magnetic properties of $\text{Fe}_x\text{Pd}_{1-x}$ and $\text{Co}_x\text{Pt}_{1-x}$ alloys have been investigated. It is shown that the temperature-dependent magnetic behaviour of alloys, composed of originally magnetic and non-magnetic elements, cannot be described properly unless the coupling between magnetic moments at magnetic atoms (Fe,Co) mediated through the interactions with induced magnetic moments of non-magnetic atoms (Pd,Pt) is included. A scheme for the calculation of the Curie temperature (T_C) for this type of systems is presented which is based on the extended Heisenberg Hamiltonian with the appropriate exchange parameters J_{ij} obtained from *ab-initio* electronic structure calculations. Within the present study the KKR Green's function method has been used to calculate the J_{ij} parameters. A comparison of the obtained Curie temperatures for $\text{Fe}_x\text{Pd}_{1-x}$ and $\text{Co}_x\text{Pt}_{1-x}$ alloys with experimental data shows rather good agreement.

PACS numbers: 71.20.Be, 75.30.Hx, 75.40.Cx

I. INTRODUCTION

Whether a magnetic material is technologically useful or not depends on its properties at finite temperatures. However, the *ab-initio* treatment of finite-temperature magnetism remains a challenge despite ongoing progress in this field during the last decades.

In this context, itinerant-electron 3d-transition metals and their alloys receive particular interest. For these systems, finite-temperature magnetic properties cannot be described successfully neither within the collective-electron Stoner model nor within the local-moment model based on the Heisenberg Hamiltonian (for an overview see Refs. [1, 2]). The Stoner model, which treats the transition to the paramagnetic state as vanishing of the local magnetic moments, accounting thereby only for the longitudinal spin fluctuations, grossly overestimates the Curie temperature T_C . A bigger success has been achieved using the Heisenberg model, which accounts for temperature-induced transverse spin fluctuations and characterizes the paramagnetic state by orientational disorder within the system of localized magnetic moments. However, a magnitude of the moments is assumed to be unchanged upon fluctuations. In some recent studies the Heisenberg model approach has been combined with *ab-initio* band-structure calculations, that allow to evaluate the exchange coupling parameters from first principles [3]. In this way, trends of the Curie or Néel temperature with composition can be quantitatively described for many systems, in particular, for transition metal monoxides [4], dilute magnetic semiconductors [5] or transition metals [6].

Despite the rather satisfying results obtained within this combined approach for several systems, the description of finite-temperature magnetism of transition metals and alloys still suffers from many problems owing to the restrictions of the Heisenberg model. For some itinerant-electron systems, e.g. Ni, the thermally-induced longitudinal spin fluctuations play a crucial role in describing properly the temperature-dependent magnetisation and obtaining the correct value for the critical temperature. A phenomenological theory of finite temperature magnetism, which accounts for both types of fluctuations on the same footing, was developed in the past [7–10]. This theory was used in combination with *ab-initio* electronic structure calculations to describe temperature dependent magnetic properties of Fe, Co and Ni [11–13]. In this way a much better agreement with experiment, as compared to calculations based on the Heisenberg model, was obtained. In particular, proper accounting for longitudinal fluctuations results in the vanishing of local magnetic moments on Ni atoms

above T_C [13], in agreement with experiment.

Other interesting itinerant-electron systems in this context are alloys or compounds composed of originally magnetic and non-magnetic elements. Such systems exhibit the so called covalent magnetism [14, 15], where magnetisation of the 'non-magnetic' atoms is governed by the spontaneously magnetised atoms via the strong spin-dependent hybridisation of their electronic states. The $\text{Fe}_x\text{Pd}_{1-x}$ and $\text{Co}_x\text{Pt}_{1-x}$ alloys considered in the present work belong to this type of systems. To describe the temperature-dependent magnetism of such systems on the basis of Heisenberg model, one obviously has to account properly for the behavior of the Pd/Pt sub-lattices. Only a few *ab-initio* studies of finite-temperature magnetism of systems of this kind have been done so far. Similarly to the work mentioned above [11–13] these studies were based on a generalisation of the classical Heisenberg Hamiltonian in one or another way to account for the different character of magnetism on different types of atoms. Mryasov et al. [16] have investigated the compound FePt and showed that the anomalous temperature-dependence of its magneto-crystalline anisotropy energy (MAE) is due to the induced Pt magnetic moments. In another study of these authors [17], a crucial role of the magnetic moment induced on Rh was demonstrated for the stabilisation of the ferromagnetic state of FeRh and for the control of the antiferromagnet-ferromagnet phase transition. Lezaic et al. [18] emphasized the need to account for longitudinal fluctuations of magnetic moments induced on Ni atoms for a proper description of the temperature-dependence of the spin-polarisation at the Fermi energy E_F in the half-metallic ferromagnet NiMnSb. Sandratskii et al. [19] investigated several ways for accounting for the induced magnetic moments within the spin-spiral approach used for the calculation of the exchange coupling parameters in NiMnSb and MnAs. Using these results Sandratskii et al. [19] have studied finite-temperature magnetic properties of NiMnSb; their findings are consistent with the findings of Lezaic et al [18].

In this work we introduce an *ab-initio* method to describe finite-temperature magnetism of systems with spontaneous and induced magnetic moments. The method is based on an extension of the Heisenberg Hamiltonian by adding a term which describes the induced magnetic moments within the linear response formalism. Our approach relies on a combination of *ab-initio* band-structure calculations with Monte Carlo (MC) simulations based on the extended Heisenberg model. To test this approach, we investigate finite-temperature magnetic properties of Pd-rich $\text{Fe}_x\text{Pd}_{1-x}$ alloys, with Fe concentrations up to 20 at.%, as

well as of ordered and disordered Co_3Pt , CoPt and CoPt_3 alloys that are interesting both for fundamental reasons and for possible use in industrial applications because of their high magnetic anisotropy [20, 21]. Theoretical investigations of finite-temperature magnetism of these systems failed so far to reproduce experimental results with satisfactory accuracy [22]. We demonstrate in the present work that a combination of *ab-initio* band-structure calculations with the Monte Carlo (MC) simulations based on the extended Heisenberg model gives satisfying agreement between theoretical and experimental values of critical temperatures. We found that despite their small magnitudes, the moments induced on non-magnetic atoms (Pd, Pt) have an important influence on finite-temperature magnetic order.

II. EXPERIMENTAL DETAILS

The $\text{Fe}_x\text{Pd}_{1-x}$ films were thermally evaporated onto oxidized silicon substrates from separate effusion cells for Pd and Fe in an ultra high vacuum system (base pressure 5×10^{-11} mbar). The film thicknesses were between 15 and 20 nm. The deposition rate of the two components could be controlled independently, resulting in an accuracy of the Fe concentration of 1%. Auger spectroscopy on a sample with nominally 7% Fe content provided an independent value of 7.8% Fe for this film. After deposition, the films were patterned into a six-terminal Hall-bar geometry. Measurements of the anomalous Hall effect at temperatures between 2K and 300 K provided the magnetization $M(T)$, from which the Curie temperatures of the films were deduced.

III. THEORETICAL APPROACH

A. Ground-state calculations

Within the present work, spin-polarised electronic structure calculations for the ground-state have been performed using the multiple scattering KKR (Korringa-Kohn-Rostoker) Green's function method [23] in the scalar-relativistic approximation. The local spin density approximation (LSDA) for density functional theory was used with the parametrisation for the exchange-correlation potential due to Vosko, Wilk, and Nusair [24]. The potential was treated within the atomic sphere approximation (ASA) with the radii of the spheres around Fe/Co and Pd/Pt sites chosen by requiring the ratios of the corresponding volumes to be the

same as for the pure elements. For the angular momentum expansion of the Green's function a cutoff of $l_{max} = 3$ was applied. For substitutionally disordered alloys, the self-consistent coherent potential approximation (CPA) method was employed. A geometry optimisation was performed, i.e., the lattice constants of the alloys have been obtained by minimisation of the total energy.

B. Extended Heisenberg Hamiltonian

The finite temperature properties of the investigated systems were studied by Monte Carlo simulations based on the Heisenberg model with the underlying Hamiltonian given by

$$H_{ex} = - \sum_{ij} \tilde{J}_{ij}^{M-M} \vec{M}_i \vec{M}_j - \sum_{ij} \tilde{J}_{ij}^{M-m} \vec{M}_i \vec{m}_j - \sum_{ij} \tilde{J}_{ij}^{m-m} \vec{m}_i \vec{m}_j . \quad (1)$$

Here the classical Hamiltonian was generalised to allow an application to itinerant-electron systems consisting of magnetic and non-magnetic atoms having magnetic moments M_i and m_i , respectively, connected with corresponding exchange coupling parameters. The dependence of the induced magnetic moments m_i on a specific magnetic configuration is treated via linear response formalism (for details see the Appendix).

We suppose that the induced magnetic moments on Pd or Pt atoms are governed only by the magnetic moments of the Fe or Co atoms in $\text{Fe}_x\text{Pd}_{1-x}$ and $\text{Co}_x\text{Pt}_{1-x}$ alloys, respectively, arranged in the first neighbor shell around the non-magnetic atom, so that

$$\vec{m}_i = \sum_{j \in M} X_{ij}^{m-M} \vec{M}_j = X_i^{m-M} \sum_{j \in M} \vec{M}_j . \quad (2)$$

The notation $\sum_{j \in M}$ means that the sum includes only such terms where j is a site with an inducing magnetic moment.

In this case (see Appendix) the susceptibility X_{ij}^{m-M} can be approximated by the value found for the ground state of a system with well defined collinear spontaneous (Fe, Co) and induced (Pd, Pt) magnetic moments:

$$X_i^{m-M} = \frac{m_i}{\sum_{j \in M} M_j} . \quad (3)$$

The exchange coupling parameters \tilde{J}_{ij} between atoms i and j in the Eq. (1) were obtained via the formula of Lichtenstein et al. [3]:

$$J_{ij} = -\frac{1}{4\pi} \text{Im} \int^{E_F} dE \text{Tr} (t_{i\uparrow}^{-1} - t_{i\downarrow}^{-1}) \tau_{\uparrow}^{ij} (t_{j\uparrow}^{-1} - t_{j\downarrow}^{-1}) \tau_{\downarrow}^{ji}. \quad (4)$$

with the relation

$$\tilde{J}_{ij} = \frac{J_{ij}}{|\vec{m}_i||\vec{m}_j|}. \quad (5)$$

In Eq. (4), $t_{i\sigma}$ and τ_{σ}^{ij} are the spin (σ) and site (i, j) dependent single-site and scattering path operator matrices occurring within the KKR formalism [25].

C. Evaluation of T_C

The Curie temperature T_C was evaluated with the Monte Carlo (MC) method [26] using the standard Metropolis importance sampling algorithm [27], on the basis of the model Hamiltonian in Eq. (1). The number of atoms in the MC unit cell for different concentrations was taken between 1728 and 4000 and T_C was determined from the peak position of the temperature-dependent susceptibility. The Fe/Co magnetic moments were treated during MC simulation as localised and changed only their orientation. On the other hand, the magnetic moments on Pd/Pt atoms could change their absolute value as well as the orientation in accordance with the changed magnetic configuration around these atoms. Eq. (2) implies that the magnetic moments on Pd/Pt are proportional to the vector sum of magnetic moments at neighboring Fe/Co atoms with only nearest neighbors taken into account. This means that each MC step consists of 1) change of the orientation of a magnetic moment on the Fe/Co atoms, 2) search for all nearest neighbour Pd/Pt atoms and calculation of the orientation and absolute value of their moments using the susceptibilities X^{m-M} via Eq. (3). The change of the energy of the total system is due to both effects. For disordered alloys the resulting T_C values in addition were averaged over up to 20 different configurations.

Obviously, the approach described above, accounts for the contribution of spin polarised 'non-magnetic' atoms to the exchange interactions between the magnetic atoms. As this contribution is temperature-dependent, it allows a corresponding description of the temperature dependent magnetisation. In particular, it accounts for longitudinal spin fluctuations

occurring on the 'non-magnetic' sub-lattice. Below it will be shown that this rather simple scheme gives rather good agreement with experimental data for the systems under consideration.

IV. RESULTS FOR $\text{Fe}_x\text{Pd}_{1-x}$ ALLOYS

A. *Ab-initio* calculations

The scheme for calculation of temperature dependent magnetic properties, described above, was used to investigate disordered $\text{Fe}_x\text{Pd}_{1-x}$ alloys with Fe concentration up to 20 at.%. The exchange coupling parameters $J_{ij}^{\text{Fe}-\text{Fe}}$ and $J_{ij}^{\text{Fe}-\text{Pd}}$, shown in Fig. 1, have a similar dependency on the distance R_{ij} for all investigated alloys. In the Pd rich limit (Fe concentration $x < 0.2$) the exchange coupling parameters $J_{ij}^{\text{Fe}-\text{Fe}}$ corresponding to the average distance between magnetic atoms is rather small and does not allow to create long-range magnetic order in the system, as was demonstrated by corresponding restricted MC simulations.

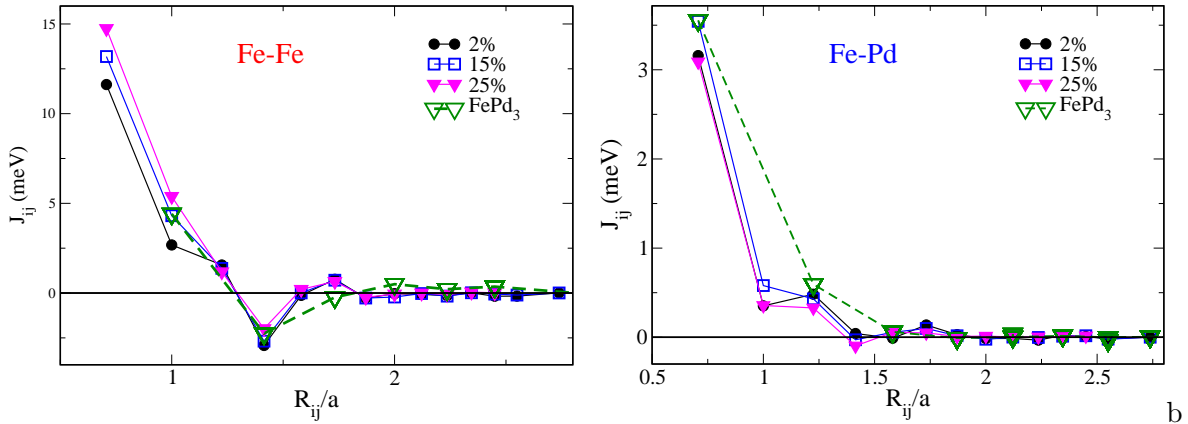


FIG. 1: Exchange coupling parameters $J^{\text{Fe}-\text{Fe}}$ (a) and $J^{\text{Fe}-\text{Pd}}$ (b) for $\text{Fe}_x\text{Pd}_{1-x}$ alloys at different concentrations. The dashed lines represent results for ordered FePd_3 (note that in this case for the Fe atoms the nearest neighbour interaction $J^{\text{Fe}-\text{Fe}}$ is absent because there are only Pd nearest neighbours).

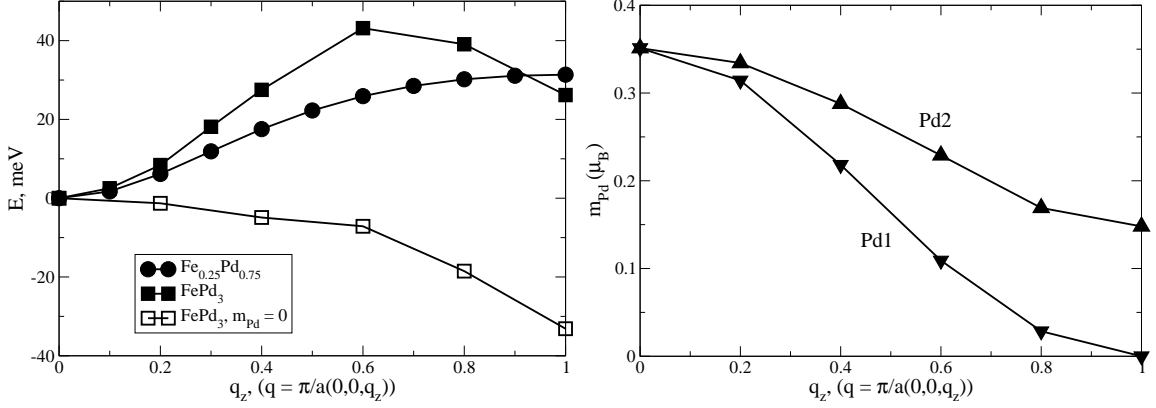


FIG. 2: Results of spin-spiral calculations for ordered FePd_3 and disordered $\text{Fe}_{0.25}\text{Pd}_{0.75}$: (a) the energy of spin spirals as a function of the wave vector $q = \frac{\pi}{a}(0,0,q_z)$, obtained for the disordered alloy (full circles), for the ordered compound with non-zero Pd magnetic moments (full squares) and for the ordered compound with Pd magnetic moments equal to 0 (open squares); (b) - magnetic moment of inequivalent Pd atoms in ordered FePd_3 as a function of the wave vector q_z . Fe and Pd2 occupy the sites $(0,0,0)$ and $(\frac{1}{2},\frac{1}{2},0)$, respectively, Pd1 atoms occupy the sites $(0,\frac{1}{2},\frac{1}{2})$ and $(\frac{1}{2},0,\frac{1}{2})$.

According to the experimental findings [28], the alloys exhibit ferromagnetic order for Fe concentrations above 0.1%. In addition, previous experimental [29–36] and theoretical [15, 37–41] investigations on the magnetic properties of $\text{Fe}_x\text{Pd}_{1-x}$ alloys have shown a strong host polarisation by magnetic Fe impurities leading to a giant magnetic moment per impurity atom, up to $12.9\mu_B$. A wide-spread regime of magnetised Pd atoms leads to ferromagnetic order in diluted $\text{Fe}_x\text{Pd}_{1-x}$ alloys despite a large distance between the magnetic Fe atoms.

The crucial role of the induced magnetic moment on Pd for the Fe-Fe exchange interactions can be demonstrated by an analysis of the energy of spin spirals as a function of a wave vector, shown in Fig. 2 for the disordered alloy $\text{Fe}_{0.25}\text{Pd}_{0.75}$ in comparison with the results for the ordered compound FePd_3 . The calculations have been performed for spin spirals along the z direction with the Fe magnetic moments tilted by 90° with respect to the z -axis. For the ordered system an increase of the wave vector of the spin spirals is accompanied first by an increase in energy reflecting the stability of the ferromagnetic order in the system. A further increase of the wave vector above $q_z > \pi/2a$, leads to a decrease of the energy of the spin spiral (Fig. 2a). This behavior is governed by a decrease of the Pd magnetic moments

at these wave vectors (see Fig. 2b), that diminishes their role in the Fe-Fe exchange.

The role of Pd becomes clearly visible for the spin spirals in FePd_3 with the Fe-Pd exchange interactions being suppressed. This can be achieved by forcing the Pd induced magnetic moments to be perpendicular to the Fe magnetic moments, and therefore to be equal to 0 (see Appendix). In this case the minimum of the spin-spiral energy corresponds to an AFM state, i.e. at $q = \pi/a$, that originates from Fe-Fe exchange interaction (see Fig. 1). In the case of the disordered alloy, the dependence of the spin-spiral energy on the wave vector is different because the random distribution of the Fe atoms allows Fe atoms to be nearest neighbours with a strong FM interaction. Due to this, the system retains the FM order at all values of wave vector \vec{q} .

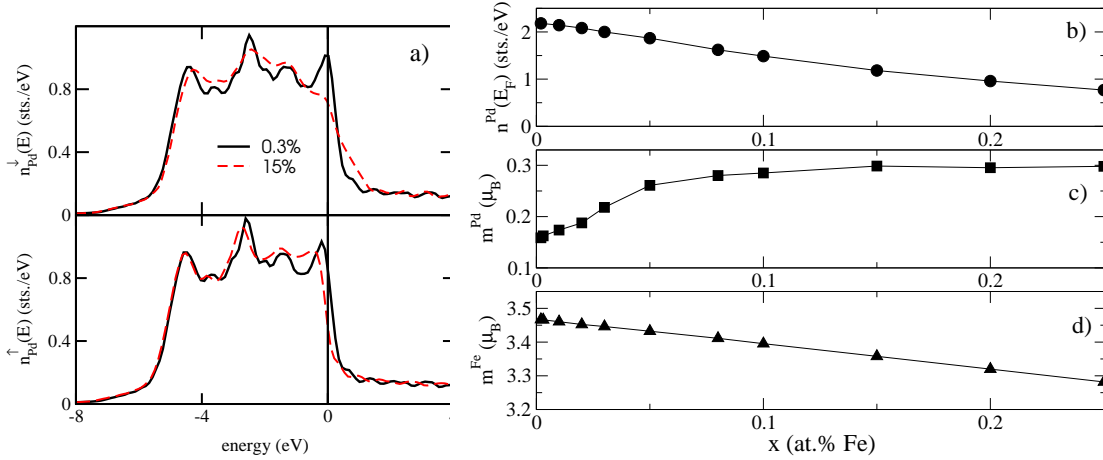


FIG. 3: a) Pd DOS in $\text{Fe}_x\text{Pd}_{1-x}$ for $x = 0.003$ and $x = 0.15$ for spin-up (upper panel) and spin-down (lower panel) states. Ground state characteristics of $\text{Fe}_x\text{Pd}_{1-x}$ alloys vs. Fe concentration: b) density of states of Pd at the Fermi level; c) Pd spin magnetic moments; d) Fe spin magnetic moments.

While the ground-state magnetic properties of $\text{Fe}_x\text{Pd}_{1-x}$ alloys can essentially be understood on the basis of *ab-initio* electronic structure calculations, a theoretical description of finite-temperature properties faces many difficulties due to the itinerant-electron nature of magnetism. Theoretical investigations based on the results of *ab-initio* electronic structure calculations have been performed for example by Mohn and Schwarz [15]. They used the model approach formulated by Bloch et al. [42] to describe the magnetic behavior of a system characterised by the coexistent local- and itinerant-electron magnetism. Within

this approach the system is characterised by two interacting subsystems: (i) one having local magnetic moments showing a Curie-Weiss-like behaviour and (ii) an itinerant electron subsystem magnetically polarised by the effective Weiss field, with the corresponding parameters found by *ab-initio* electronic structure calculations.

The spin moment on every Pd atom is induced by the magnetic moment of the Fe atoms and all surrounding induced Pd magnetic moments (see Appendix). The rather big absolute value and large region of Pd induced magnetic moments around an Fe atom is a result of the high magnetic spin susceptibility of pure Pd and $\text{Fe}_x\text{Pd}_{1-x}$ alloys with small Fe concentration, that is determined by a large Pd density of states (DOS) at the Fermi level, $n(E_F)$ (see Fig. 3a). In turn, $n(E_F)$ decreases with the increase of Fe content in the alloy (Fig. 3b), resulting in a decrease of the partial magnetic susceptibility of the Pd atoms. Thus, at very small Fe concentrations the induced Pd spin moment can extend to big distances - inducing shell-by-shell a spin moment in the Pd subsystem. This polarisation mechanism decays with the distance from the magnetic impurity. When the Fe concentration increases, the regions with the induced moments overlap and, as was pointed in M. Shimizu et al. [43, 44], when the Fe concentration is larger than 0.1% the Pd magnetic properties can be described well by band calculations, as done in our present calculations using the CPA alloy theory.

Figure 3, c and d, represent the spin magnetic moments of Pd and Fe versus the Fe content in $\text{Fe}_x\text{Pd}_{1-x}$. As is seen, the Fe magnetic moments change only slowly with the increase of Fe concentration, while the variation of the Pd spin magnetic moments is rather pronounced. This can be directly connected to the decrease of the Pd DOS at the Fermi level.

For a more detailed analysis, we investigated the properties of the induced Pd magnetic moment using the *ab-initio* calculations. In particular, we studied the distribution of the Pd magnetic moment in a Pd host in the limit of very small Fe concentrations, i.e. around a single Fe impurity. To see that the induced magnetic moment at every Pd atom is determined not only by the Fe magnetic moment but also by the surrounding Pd magnetic moments, one can compare the un-enhanced induced Pd spin moments created by only one Fe atom with the total induced spin moments in Pd. The total induced magnetic moment distribution in Pd can be found by solving the system of equations (A3) within a selected region around an

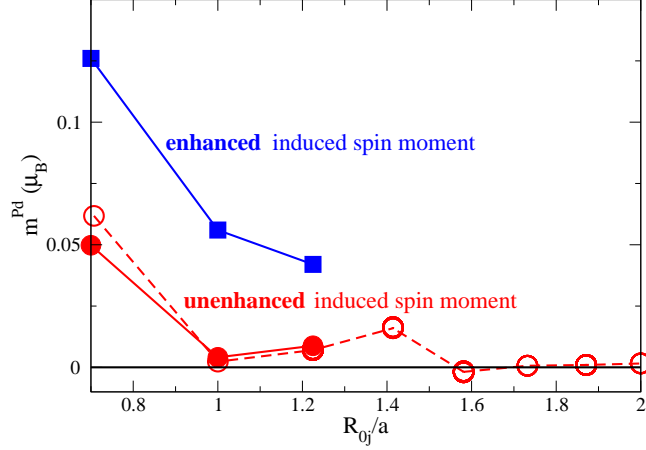


FIG. 4: Magnetic moment distribution in Pd around a single Fe impurity, as a function of the distance from the magnetic atom. Full squares represent the Pd magnetic moments self-consistently obtained within a cluster with 3 atomic shells of Pd around an Fe impurity embedded into a Pd host, full circles give the results obtained for the same system but with the exchange potential switched off. The open circles represent the induced magnetic moments in Pd calculated within linear response formalism using Eq. (A1) in the Appendix.

Fe atom (see Appendix). In addition, in the present work the moment distribution has been obtained by self-consistent electronic structure calculations instead of using linear response formalism. Fig. 4 shows the slow decay of the induced magnetic moment with the distance (full squares). The corresponding un-enhanced induced moment in these calculations has been obtained by suppressing the effective exchange B-field for the Pd atoms during the SCF-cycle. These un-enhanced magnetic moments compare very well with those obtained from linear response formalism (Eq. (A1)) (open circles). These are shown in Fig. 4 also for larger distances. One can see that the decrease with the distance of the Pd un-enhanced spin moment is very fast compared to the enhanced one. For the nearest Pd neighbors of Fe atom these values differ approximately by a factor of 2, while the difference for the next nearest neighbors is already an order of magnitude. The local exchange enhancement, well approximated within the linear approach at small values of the induced magnetic moments, should keep the ratio of these two values approximately constant. The obtained results give evidence for a more complicated picture of the creation of the induced magnetic moment in accordance to the description given in the Appendix.

The effect of temperature-induced magnetic disorder within the Fe-subsystem was anal-

used within *ab-initio* calculations, describing magnetic disorder within the uncompensated Disordered Local Moment (DLM) approximation. Using this approximation an effective alloy of two types of Fe atoms with opposite spin directions and having different concentrations is treated using the CPA alloy theory. In this way one can study the dependence of the induced magnetic moment of individual Pd atoms on the average magnetic moment in the system. Fig. 5 shows that the magnetic disorder in the Fe subsystem (assumed to be temperature induced) is accompanied by a decrease of the total magnetic moment in the system and results in a decrease of the induced magnetic moment in the Pd subsystem. One can see a rather good linear dependence of the induced Pd magnetic moment as a function of the magnetic moment of the Fe subsystem, for nearly all Fe concentrations. Only in the limiting case of low Fe concentration (1%), a noteworthy deviation from linear behavior is observed. This deviation will influence the final results in a Curie temperature evaluation correspondingly.

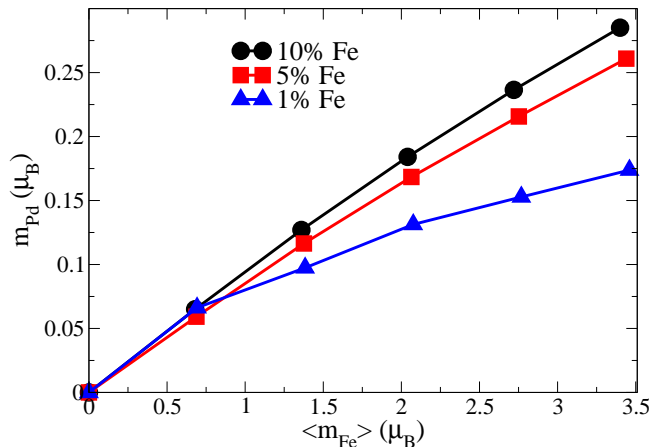


FIG. 5: Results of *ab-initio* calculations for induced Pd moment in three Fe-Pd alloys, using the uncompensated DLM approximation as a function of the Fe average magnetic moment.

B. Finite-temperature magnetism of $\text{Fe}_x\text{Pd}_{1-x}$ alloys

The temperature dependent magnetic properties of $\text{Fe}_x\text{Pd}_{1-x}$ alloys were investigated by performing Monte Carlo simulations. They show an absence of an ordered FM state for the alloys with Fe concentration up to $x \approx 0.2$ if the Fe-Fe exchange interactions mediated

by Fe-Pd interactions are neglected. This clearly demonstrates the importance of these interactions. The Curie temperature for disordered $\text{Fe}_{0.2}\text{Pd}_{0.8}$ alloy in this case is around 60K, much lower than observed experimentally (around 400 K). To illustrate the role of Fe-Pd interactions in the formation of magnetic order, Fig. 6 shows spin configurations obtained within MC simulations for ($T = 0.1\text{K}$) for the $\text{Fe}_x\text{Pd}_{1-x}$ alloy with $x = 0.02$. Fig. 6a represents a result for the case that the Fe-Pd exchange interactions are neglected and therefore it shows only the magnetic moments of Fe. Fig. 6b represents the spin configuration when the Fe-Pd first-neighbour interactions are taken into account and shows only those Fe and Pd magnetic moments which give a contribution to the total energy of a system given by Eq. (1).

A comparison of T_C obtained within the MC simulation based on the Hamiltonian in Eq. (1) with the experimental data for $\text{Fe}_x\text{Pd}_{1-x}$ alloys is shown in Fig. 7. Obviously, a rather good agreement is obtained for the whole concentration range. It should be emphasized once more that all parameters for the model Hamiltonian (Eq. (1)) are obtained within *ab-initio* electronic structure calculations using the scheme described in the Appendix. Of course, going beyond the various approximations the final results can be improved to get better agreement with the experimental results. Fig. 7 shows that the theoretical result obtained by Mohn and Schwarz [15] for $\text{Fe}_x\text{Pd}_{1-x}$ alloys at small Fe concentrations is also in a good agreement with experiment. However, it should be emphasized that this work is based on a semi-phenomenological approach.

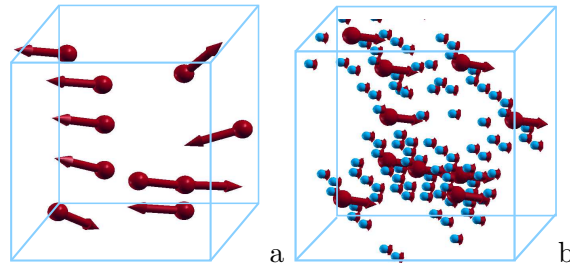


FIG. 6: The distribution of spin moments in unit cell used within the MC simulations without (a) and with (b) the induced Pd moments taken into account. Large arrows correspond to the Fe magnetic moments, small arrows to Pd magnetic moments.

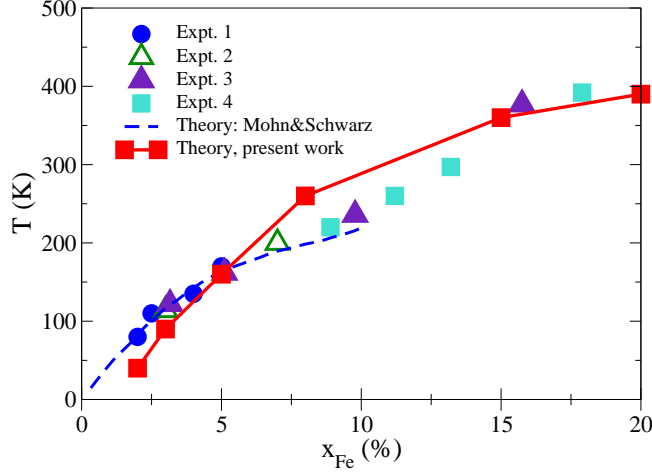


FIG. 7: (a) The Curie temperature for different Fe concentrations in $\text{Fe}_x\text{Pd}_{1-x}$ alloys: present results vs theoretical results of Mohn and Schwarz [15] and experimental data: Expt. 1 – present work, Expt. 2 [30], Expt. 3 [34], Expt. 4 [45].

system		a	$\mu_{\text{spin}} (\text{Co})$	$\mu_{\text{spin}} (\text{Pt})$
		a.u.	μ_B	μ_B
Co_3Pt	ordered	6.98	1.82	0.36
	disordered	7.06	1.88	0.25
CoPt	ordered	7.23	1.93	0.37
	disordered	7.23	2.03	0.27
CoPt_3	ordered	7.31	1.76	0.26
	disordered	7.37	2.19	0.25

TABLE I: Equilibrium lattice constants and magnetic moments at Co and Pt atoms for ordered and disordered $\text{Co}_x\text{Pt}_{1-x}$ alloys.

V. RESULTS FOR $\text{Co}_x\text{Pt}_{1-x}$ ALLOYS

A. Magnetic moments and exchange coupling constants

The calculated equilibrium lattice constants for ordered and disordered $\text{Co}_x\text{Pt}_{1-x}$ alloys are shown in Tab. I. For ordered CoPt , we used a simplified $L1_0$ geometry, assuming $c=a$ instead of $c=0.98a$ found in experiment. The magnetic moments of the Co and Pt atoms for the equilibrium lattice constants obtained in the scalar-relativistic mode are presented

in Table I. More details about ground-state properties of Co-Pt can be found in our earlier study [46].

The exchange coupling constants J_{ij} for the investigated systems were evaluated via Eq. (4). The dependence of J_{ij} on the distance between the atoms i and j is displayed in Fig. 8 with the left panels showing the situation when both i and j are Co atoms and the right panels showing the situation when i is a Co atom and j is a Pt atom. If experimental lattice constants were used instead of equilibrium lattice constants, the J_{ij} constants would change slightly but both the trends and the values would remain similar as in Fig. 8.

One can see from Fig. 8 that for Co_3Pt and CoPt the coupling between the moments on the Co atoms do not differ very much from the results for their disordered counterparts, $\text{Co}_{0.75}\text{Pt}_{0.25}$ and $\text{Co}_{0.50}\text{Pt}_{0.50}$ respectively. However, the situation changes dramatically for CoPt_3 (lower left panel in Fig. 8). The pronounced difference between the data for the ordered and the disordered system stems mainly from the fact that there are no Co atoms present for some coordination spheres around a central Co atom in ordered CoPt_3 . Concerning the coupling between moments on Co and Pt atoms, the degree of long-range order has a larger influence than for the Co-Co coupling. For ordered alloys, the J_{ij} constants significantly vary also with composition. For disordered alloys, on the other hand, the J_{ij} constants do not vary very much with composition. For ordered CoPt_3 , there is a surprisingly strong Co-Co coupling between atoms which are $2.83\ a$ apart. We verified that for larger distances no comparable strong coupling occurs.

B. Curie temperatures

The Curie temperatures T_C of the investigated Co-Pt systems evaluated by means of the Monte-Carlo technique are shown in Tab. II. In addition, results for fcc Co are given in this table. The two theoretical Curie temperatures correspond to two different Hamiltonians used to describe the magnetic coupling. The first T_C (denoted as “Co-Co only” in Tab. II) corresponds to the standard Heisenberg Hamiltonian for magnetic moments only on the Co atoms. The second T_C (denoted as “Co-Co and Co-Pt”) corresponds to the extended Heisenberg Hamiltonian (Eq. (1)), accounting for the coupling between moments on Co atoms $\tilde{J}_{ij}^{\text{Co-Co}}$ as well as for the coupling between moments on Co and Pt atoms $\tilde{J}_{ij}^{\text{Co-Pt}}$, with the moments on Pt atoms determined via Eqs. (2) and (3). The values of T_C obtained

system	model	T_C [K]	T_C [K]
		ordered	disordered
fcc Co	MC	1100	
	experiment	1388	
	Mohn-Wohlfarth	3523	
Co ₃ Pt	MC, Co-Co only	800	750
	MC, Co-Co and Co-Pt	900	880
	experiment	–	1100
	Mohn-Wohlfarth	1803	1120
CoPt	MC, Co-Co only	360	620
	MC, Co-Co and Co-Pt	620	760
	experiment	727	830
	Mohn-Wohlfarth	1964	850
CoPt ₃	MC, Co-Co only	–180	370
	MC, Co-Co and Co-Pt	150	520
	experiment	288	468
	Mohn-Wohlfarth	241	510

TABLE II: Curie temperatures T_C for fcc Co and for ordered and disordered Co_xPt_{1-x} alloys. Experimental results [47, 48] are shown together with results of our Monte-Carlo calculations with either both Co-Co and Co-Pt coupling or with only Co-Co coupling included. For comparison, results obtained by relying on the Mohn-Wohlfarth theory are also shown [22, 49, 50]. Negative T_C implies antiferromagnetic ordering.

earlier by relying on the semi-empirical Mohn-Wohlfarth theory [51] were taken from Qi et al. [49] for fcc Co, from Kashyap et al. [22] for ordered Co-Pt compounds and from Ghosh et al. [50] for disordered Co_xPt_{1-x} alloys. Experimental values [47, 48] are shown for comparison. Note that an experimental value for T_C for ordered Co₃Pt is not available because the ordered phase is not stable for this composition.

As is seen, the Mohn-Wohlfarth theory [51] gives reasonable agreement with experiment at small Co concentration. However, increasing the Co content leads to large discrepancies

between the theory and experiment. This results from the limitations of the Mohn-Wohlfarth theory: it was developed for homogeneous itinerant-electron systems, which is not the case for $\text{Co}_x\text{Pt}_{1-x}$ alloys.

Our *ab-initio* scheme based on an extended Heisenberg Hamiltonian (both Co-Co and Co-Pt coupling included) accounts quantitatively for the trends of T_C with the composition and with the degree of long-range order. If the coupling mediated via moments at Pt atoms is not included, the results are unrealistic. This is especially true for ordered CoPt_3 , where an *antiferromagnetic* order is established at finite temperatures (reflected by a negative value for T_C) if the coupling between moments on Co and Pt is ignored.

VI. CONCLUSIONS

As was shown in the present work by the examples of $\text{Fe}_x\text{Pd}_{1-x}$ and $\text{Co}_x\text{Pt}_{1-x}$ alloys, the finite-temperature magnetism of alloys composed of magnetic and non-magnetic elements requires to account for the exchange interactions between magnetic atoms, mediated by the exchange interaction with non-magnetic atoms. This implies in particular that one has to account properly for the induced magnetic moment within the Monte Carlo simulations which are based in the present work on a corresponding extension of the standard Heisenberg Hamiltonian. The approach presented suggests to describe the induced magnetic moment on non-magnetic atoms within linear response formalism, being proportional to the vector sum of magnetic moments of neighboring magnetic atoms. This ansatz allows for substantial technical simplifications and leads to substantial improvement of the results when compared to simpler schemes.

The finite-temperature calculations for $\text{Fe}_x\text{Pd}_{1-x}$ and $\text{Co}_x\text{Pt}_{1-x}$ alloys performed within this approach give the dependence of T_C on the composition as well as on the degree of long-range order in good agreement with experimental data. The case of ordered CoPt_3 also demonstrates that even if the coupling between nearest inducing moments is antiferromagnetic, the magnetic order can still be ferromagnetic due to the effect of coupling between inducing and induced moments. A mere inspection of the J_{ij} constants thus cannot serve as a reliable indicator of ferromagnetic or antiferromagnetic order at $T \neq 0K$.

VII. ACKNOWLEDGEMENT

This work was supported by the DFG within the SFB 689 "Spinphänomene in reduzierten Dimensionen" as well as the project Eb 154/20 "Spin polarisation in Heusler alloy based spintronics systems probed by SPINAXPES", and by GA CR within the project 202/08/0106.

Appendix A: Induced magnetic moments

The magnetic moment induced on site i (Pd or Pt) by the exchange field \vec{B}_j^{xc} due to magnetic moments at site j can be calculated within the linear response formalism using the expression [52]:

$$\begin{aligned}\vec{m}_i^0(\vec{r}) &= -\frac{1}{\pi}Im \int^{E_F} dE Tr \vec{\sigma} \\ &\times \int_{\Omega_j} d^3r' G(\vec{r}, \vec{r}', E) H_j^{xc}(\vec{r}') G(\vec{r}', \vec{r}, E) \\ &= \int_{\Omega_j} \chi_{ij}(\vec{r}, \vec{r}') \vec{B}_j^{xc}(\vec{r}') d^3r'\end{aligned}\tag{A1}$$

Here $H_j^{xc}(\vec{r}') = \vec{\sigma} \vec{B}_j^{xc}(\vec{r}') = \vec{\sigma} \vec{e}_M B_j^{xc}(\vec{r}')$ with $\vec{\sigma}$ - the matrix of Pauli matrices [53], \vec{e}_M the unit vector in the direction of spontaneous magnetic moment of atom j , $B_j^{xc}(\vec{r})$ the local exchange field at the site j . Note that, neglecting relativistic effects, the magnetic moment \vec{m}_i^0 induced by a neighboring magnetic atom is parallel to the direction \vec{e}_M of the magnetic moment \vec{M}_j of this atom.

The total induced magnetic moments on a Pd or Pt atom is represented as a response to the exchange field of all surrounding atoms by the following expression:

$$\begin{aligned}\vec{m}_i(\vec{r}) &= \sum_{j \in M} \int_{\Omega_j^M} \chi_{ij}^{m-M}(\vec{r}, \vec{r}') \vec{B}_j^{xc, M}(\vec{r}') d^3r' \\ &+ \sum_{j \in m} \int_{\Omega_j^m} \chi_{ij}^{m-m}(\vec{r}, \vec{r}') \vec{B}_j^{xc, m}(\vec{r}') d^3r' \\ &+ \chi_i^0(\vec{r}) \vec{B}_i^{xc, m}(\vec{r}).\end{aligned}\tag{A2}$$

Analogous to $\sum_{j \in M}$ defined at Eq. (2), the sum $\sum_{j \in m}$ means summation over sites with induced magnetic moments.

This can be reformulated in terms of local magnetic moments M_i of Fe (Co) and m_i of Pd (Pt)

$$m_i = \sum_{j \in M} \tilde{\chi}_{ij}^{m-M} \vec{M}_j + \sum_{j \in m} \tilde{\chi}_{ij}^{m-m} \vec{m}_j + \tilde{\chi}_{ii} \vec{m}_i \quad (\text{A3})$$

with

$$\vec{M}_i = \int_{\Omega_{WS}} d^3r \vec{M}_i(\vec{r}); \quad \vec{m}_i = \int_{\Omega_{WS}} d^3r \vec{m}_i(\vec{r}). \quad (\text{A4})$$

Here we use the following reformulation for the first term in Eq. (A2), that is more convenient for the model implementation:

$$\begin{aligned} & \int_{\Omega_j^M} \chi_{ij}^{m-M}(r, r') \vec{B}_j^{xc, M}(r') d^3r' \\ &= \vec{M}_j \int_{\Omega_j^M} \chi_{ij}^{m-M}(r, r') \frac{\vec{B}_j^{xc, M}(r')}{M_j} d^3r' \\ &= \tilde{\chi}_{ij}^{m-M} \vec{M}_j \end{aligned} \quad (\text{A5})$$

For the second term, using a linearised expression for the exchange potential in the case of a small induced magnetic moment on Pd and Pt sites [52, 54], one can write analogously:

$$\begin{aligned} & \int_{\Omega_j^m} \chi_{ij}^{m-m}(r, r') \vec{B}_j^{xc, m}(r') d^3r' \\ &= \vec{m}_j \int_{\Omega_j^m} \chi_{ij}^{m-m}(r, r') \frac{\delta V_j^{xc}[n, m]}{\delta m(\vec{r})} \Big|_{m_{spin}=0} \frac{m_j(\vec{r})}{m_j} d^3r' \\ &= \tilde{\chi}_{ij}^{m-m} \vec{m}_j. \end{aligned} \quad (\text{A6})$$

Solving the system of equations (A3) for a restricted region around a magnetic impurity atom gives the distribution of the induced magnetic moments on the non-magnetic atoms. This can be done for the ground state ($T = 0\text{K}$). Alternatively, without any approximations, one can get these values within *ab-initio* calculations for embedded magnetic atoms by using the CPA alloy theory, assuming an uniform distribution of the induced magnetic moment.

Strictly spoken, one can go beyond the linear approximation in the expansion of the exchange potential. However, the linear approximation makes the use of this scheme in subsequent Monte Carlo simulations much easier.

By making an additional simplification one can restrict to one response function X_{ij}^{m-M} within the Monte-Carlo simulations. This quantity is defined to give the induced magnetic moment as a response to the exchange fields of only the surrounding nearest neighbour magnetic atoms:

$$\vec{m}_i = \sum_{j \in M} X_{ij}^{m-M} \vec{M}_j. \quad (\text{A7})$$

-
- [1] J. Kübler, *Theory of itinerant electron magnetism* (Oxford University Press, Oxford, 2000), p. 460.
 - [2] P. Mohn, *Magnetism in the Solid State* (Springer, Berlin, 2003), p. 215.
 - [3] A. I. Liechtenstein, M. I. Katsnelson, V. P. Antropov, and V. A. Gubanov, J. Magn. Magn. Materials **67**, 65 (1987).
 - [4] G. Fischer, M. Däne, A. Ernst, P. Bruno, M. Lüders, Z. Szotek, W. Temmerman, and W. Hergert, Phys. Rev. B **80**, 014408 (2009).
 - [5] T. Fukushima, K. Sato, H. Katayama-Yoshida, and P. H. Dederichs, Jap. J. Appl. Phys. **43**, L1416 (2004).
 - [6] I. Turek, J. Kudrnovský, V. Drchal, P. Bruno, and S. Blügel, phys. stat. sol. (b) **236**, 318 (2003).
 - [7] J. Hubbard, Phys. Rev. B **19**, 2626 (1979).
 - [8] T. Moriya, *Spin Fluctuations in Itinerant Electron Magnetism* (Springer, Berlin, 1985).
 - [9] H. Hasegawa, J. Phys. Soc. Japan **46**, 1504 (1979).
 - [10] V. Korenman, J. L. Murray, and R. E. Prange, Phys. Rev. B **16**, 4032 (1977).
 - [11] M. Uhl and J. Kübler, Phys. Rev. Lett. **77**, 334 (1996), URL <http://link.aps.org/doi/10.1103/PhysRevLett.77.334>.
 - [12] N. M. Rosengaard and B. Johansson, Phys. Rev. B **55**, 14975 (1997).

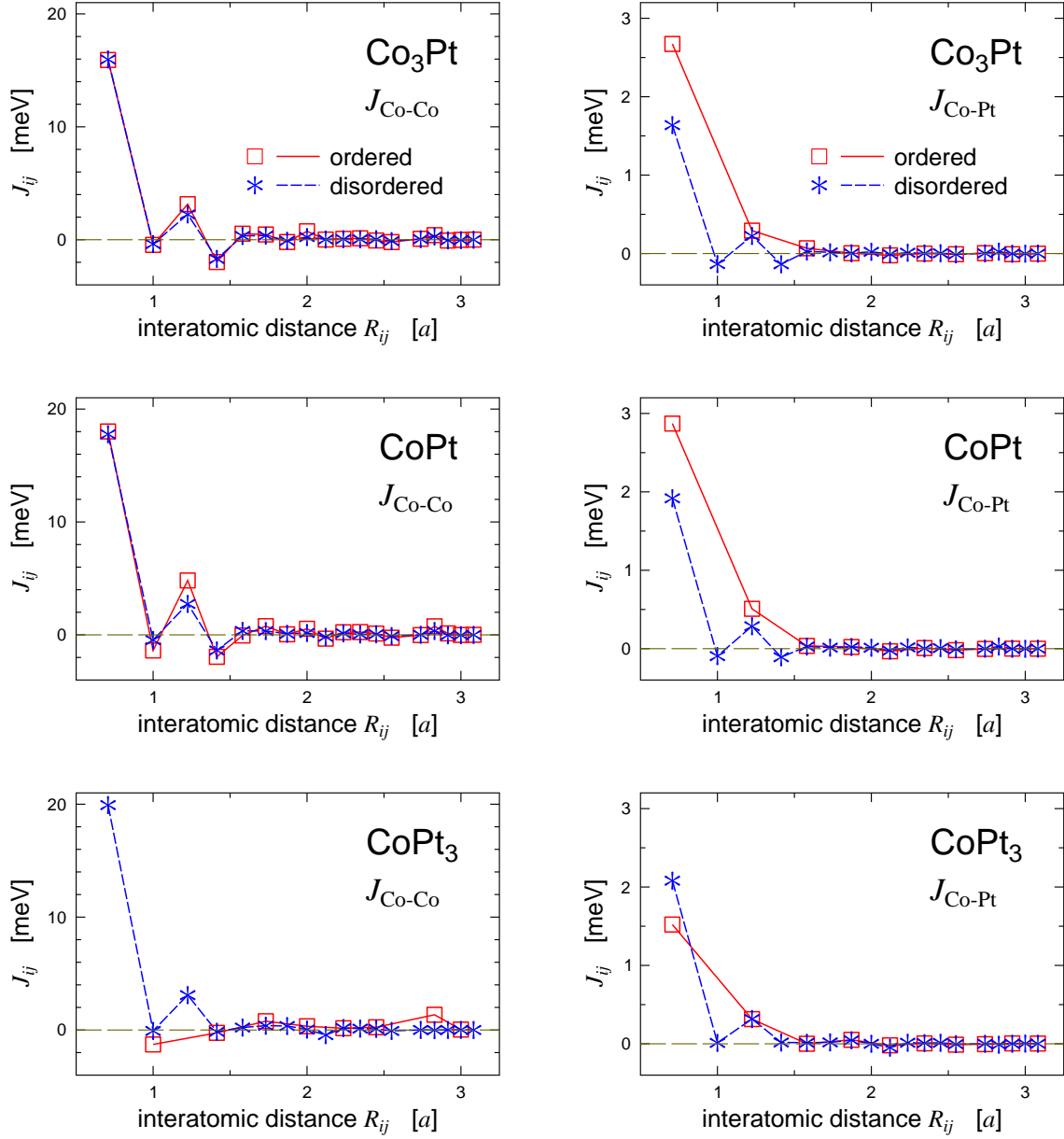


FIG. 8: Exchange coupling constants J_{ij} between moments of a Co atom on site i and on other surrounding Co atoms (j) (left panels) and between moments on a Co atom (i) and on surrounding Pt atoms (j) (right panel), for ordered and disordered $\text{Co}_x\text{Pt}_{1-x}$ alloys. The horizontal axis shows the distance R_{ij} between i and j atoms in units of lattice constants.

- [13] A. V. Ruban, S. Khmelevskyi, P. Mohn, and B. Johansson, Phys. Rev. B **75**, 054402 (2007).
- [14] A. R. Williams, R. Zeller, V. L. Moruzzi, C. D. Gelatt, and J. Kubler, J. Appl. Phys. **52**, 2067 (1981).
- [15] P. Mohn and K. Schwarz, J. Phys.: Condens. Matter **5**, 5099 (1993).
- [16] O. N. Mryasov, U. Nowak, K. Y. Gusliencko, and R. W. Chantrell, Europhys. Lett. **69**, 805 (2005).
- [17] O. N. Mryasov, Phase Transitions **78**, 197 (2005).
- [18] M. Lezaic, P. Mavropoulos, J. Enkovaara, G. Bihlmayer, and S. Blügel, Phys. Rev. Lett. **97**, 026404 (2006).
- [19] L. M. Sandratskii, R. Singer, and E. Şaşıoğlu, Phys. Rev. B **76**, 184406 (2007).
- [20] J. A. Christodoulides, Y. Huang, Y. Zhang, G. C. Hadjipanayis, I. Panagiotopoulos, and D. Niarchos, J. Appl. Phys. **87**, 6938 (2000).
- [21] G. Moulas, A. Lehnert, S. Rusponi, J. Zabloudil, C. Etz, Ouazi, M. Etzkorn, P. Bencok, P. Gambardella, P. Weinberger, et al., Phys. Rev. B **78**, 214424 (2008).
- [22] A. Kashyap, K. B. Garg, A. K. Solanki, T. Nautiyal, and S. Auluck, Phys. Rev. B **60**, 2262 (1999).
- [23] H. Ebert, in *Electronic Structure and Physical Properties of Solids*, edited by H. Dreyssé (Springer, Berlin, 2000), vol. 535 of *Lecture Notes in Physics*, p. 191.
- [24] S. H. Vosko, L. Wilk, and M. Nusair, Can. J. Phys. **58**, 1200 (1980).
- [25] P. Weinberger, *Electron Scattering Theory for Ordered and Disordered Matter* (Oxford University Press, Oxford, 1990).
- [26] K. Binder, Rep. Prog. Phys. **60**, 487 (1997).
- [27] D. P. Landau and K. Binder, *A Guide to Monte Carlo simulations in statistical physics* (Cambridge University Press, Cambridge, 2000).
- [28] J. Crangle and W. R. Scott, J. Appl. Phys. **36**, 921 (1965).
- [29] V. D. Gerstenberg, Annalen der Physik **7**, 236 (1958).
- [30] J. W. Cable, E. O. Wollan, and W. C. Koehler, Phys. Rev. **138**, A755 (1965).
- [31] P. P. Craig, B. Mozer, and S. Romeo, Phys. Rev. Lett. **14**, 895 (1965).
- [32] G. Longworth, Phys. Rev. **172**, 572 (1968).
- [33] G. Chouteau and R. Tournier, Journal de Physique C **32**, 1002 (1971).
- [34] J. Crandle, Philosophical Magazine **5**, 335 (1960).

- [35] B.-H. Yen and J. Chen, Chinese Journal of Physics **13**, 1 (1975).
- [36] J. F. van Acker, P. W. J. Weijs, J. C. Fuggle, K. Horn, W. Wilke, H. Haak, H. Saalfeld, H. Kühlenbeck, W. Braun, G. P. Williams, et al., Phys. Rev. B **38**, 10463 (1988).
- [37] D.-K. Kim, Phys. Rev. **149**, 434 (1966).
- [38] G. Bergmann, Phys. Rev. B **23**, 3805 (1981).
- [39] R. Medina and R. E. Parra, J. Appl. Phys. **53**, 2201 (1982).
- [40] C. Jian-Wang, L. He-Lie, Z. Zhi, and Z. Qing-Qi, Phys. Rev. B **5**, 5343 (1993).
- [41] A. Oswald, R. Zeller, and P. H. Dederichs, Phys. Rev. Lett. **56**, 1419 (1986).
- [42] D. Bloch, D. M. Edwards, M. Shimizu, and J. Voiron, Journal of Physics F: Metal Physics **5**, 1217 (1975).
- [43] T. Takanashi and M. Shimizu, J. Phys. Soc. Japan **20**, 26 (1965).
- [44] M. Shimizu and T. Kato, Phys. Lett. **27A**, 166 (1968).
- [45] B.-H. Yeh, J. Chen, P. K. Tseng, and S.-H. Fang, Chinese J. Phys **13**, 1 (1975).
- [46] O. Šipr, J. Minár, S. Mankovsky, and H. Ebert, Phys. Rev. B **78**, 144403 (2008), URL <http://link.aps.org/doi/10.1103/PhysRevB.78.144403>.
- [47] C. E. Dahmani, Ph.D. thesis, Louis Pasteur University, Strasbourg (1985).
- [48] M. C. Cadeville, C. E. Dahmani, and F. Kern, J. Magn. Magn. Materials **55-57**, 1055 (1986).
- [49] Q. Qi, R. Skomski, and J. M. D. Coey, J. Phys.: Condens. Matter **6**, 3245 (1994).
- [50] S. Ghosh, C. B. Chaudhuri, B. Sanyal, and A. Mookerjee, J. Magn. Magn. Materials **234**, 100 (2001).
- [51] P. Mohn and E. P. Wohlfarth, J. Phys. F: Met. Phys. **17**, 2421 (1987).
- [52] M. Deng, H. Freyer, J. Voithländer, and H. Ebert, J. Phys.: Cond. Mat. **13**, 8551 (2001).
- [53] M. E. Rose, *Relativistic Electron Theory* (Wiley, New York, 1961).
- [54] S. Mankovsky and H. Ebert, Phys. Rev. B **74**, 54414 (2006).